NLO predictions for $Wb\bar{b}$ production via double parton scattering at the LHC

Edmond L. Berger

High Energy Physics Division, Argonne National Laboratory, Argonne, IL 60439 USA

DOI: http://dx.doi.org/10.3204/DESY-PROC-2012-03/12

Next-to-leading order predictions in perturbative QCD are presented of various differential distributions for $pp \to Wb\bar{b}X \to \ell\nu b\bar{b}X$ at the Large Hadron Collider energy 7 TeV. Included are the contributions from both single parton scattering and double parton scattering as well as relevant backgrounds. Several kinematic variables are proposed for isolating the double parton contribution with the first 10 fb^{-1} of integrated luminosity. Smearing associated with next-to-leading order contributions is important for a proper description of some of the observables we compute. Under specified conditions, the double parton process can be identified and measured with signal over background significance $S/\sqrt{B} \sim 10$. The work summarized here was done in collaboration with Chris Jackson, Seth Quackenbush, and Gabe Shaughnessy.

1 Introduction

With its higher energies and larger luminosities, the Large Hadron Collider (LHC) makes it possible to investigate unexplored aspects of established theories such as quantum chromodynamics (QCD). The standard single parton scattering (SPS) picture of hadron-hadron collisions is shown on the left side of Fig. 1. One parton from each proton participates in the hard scattering to produce the final state. In SPS, the differential hadronic cross section factors:

$$d\sigma_{pp}^{SPS} = \sum_{i,j} \int f_p^i(x_1,\mu) f_p^j(x'_1,\mu) d\hat{\sigma}_{ij}(x_1,x'_1,\mu) dx_1 dx'_1 \,. \tag{1}$$

The short-distance partonic cross section $d\hat{\sigma}_{ij}$ is computed in perturbation theory, whereas the parton distribution functions (PDF) $f_p^i(x_i,\mu)$ are nonperturbative objects extracted from experiment and evolved to the appropriate hard scale μ.

The full description of hadronic collisions involves other elements including initial- and final-state soft radiation, underlying events, and multiparton interactions. Double parton scattering (DPS) describes the case in which two short-distance subprocesses occur in a given hadronic interaction, with two initial partons being active from each of the incident protons. The general picture of DPS is shown on the right side of Fig. 1. Given the small probability for single parton scattering in hadronic collisions, it is often assumed that the effects of double (or multiple) parton scattering may be ignored or subsumed into the parametrization of the underlying event. Nevertheless, it is worth exploring theoretically and investigating experimentally whether a second distinct hard component may be identified in events at the LHC. Evidence for DPS

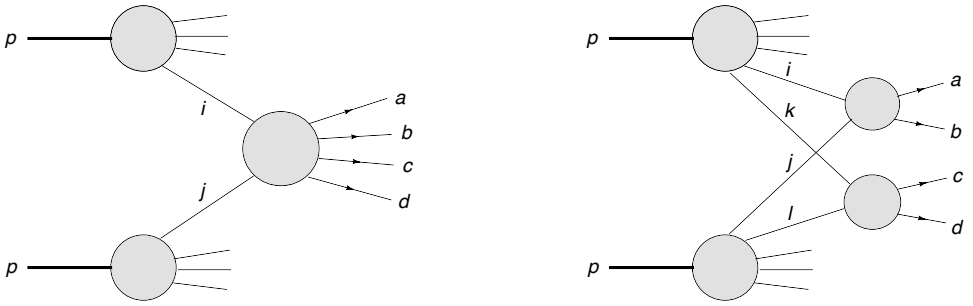

Figure 1: Schematic depiction of single parton scattering (left) and double parton scattering (right).

is reported in Refs. [1, 2, 3, 4], and many references to theoretical work may be found in Refs [5, 6, 7, 8].

In Ref. [5], we investigated the DPS and SPS contributions at the LHC for the four-parton final state $pp \to b\bar{b}jjX$ in which a $b\bar{b}$ system is produced along with two jets j. We showed that there are characteristic regions of phase space in which the DPS events are expected to concentrate, and we developed a methodology to measure the effective size of the DPS signal. Precise measurements of DPS at the LHC will provide insight into QCD dynamics beyond SPS and into parton-parton correlations, and it will help to validate a second hard component in underlying event modeling. In this contribution I summarize our next-to-leading order study in perturbative QCD of $pp \to Wb\bar{b}X \to \ell\nu b\bar{b}X$ at the Large Hadron Collider energy 7 TeV [6].

Under the assumption of weak dynamic and kinematic correlations between the two hard-scattering subprocesses, a typical approach in DPS studies is to assume the differential hadronic cross section takes a factored form in analogy to Eq. (1):

$$\begin{aligned} d\sigma_{pp}^{DPS} &= \frac{m}{2\sigma_{\rm eff}} \sum_{i,j,k,l} \int H_p^{ik}(x_1, x_2, \mu_A, \mu_B) H_p^{jl}(x_1', x_2', \mu_A, \mu_B) \\ &\quad \times d\hat{\sigma}_{ij}(x_1, x_1', \mu_A) d\hat{\sigma}_{kl}(x_2, x_2', \mu_B) dx_1 dx_2 dx_1' dx_2' \,, \end{aligned} \tag{2}$$

where m is a symmetry factor equal to 1 (2) if the two hard-scattering subprocesses are identical (nonidentical). The joint probabilities $H_p^{ik}(x_1, x_2, \mu_A, \mu_B)$ can be approximated as the product of two single PDFs:

$$H_p^{ik}(x_1, x_2, \mu_A, \mu_B) = f_p^i(x_1, \mu_A) f_p^k(x_2, \mu_B) \,. \tag{3}$$

Given that one hard scattering has taken place, the parameter $\sigma_{\rm eff}$ measures the size of the partonic core in which the flux of accompanying short-distance partons is confined. Typical values in phenomenological studies focus on the 10-12 mb region, consistent with measurements from the Tevatron collider [3, 4]. In writing Eqs. (2) and (3), we ignore possible strong correlations in longitudinal momentum. However, for the small values of x expected at the LHC, this should be a good approximation [5]. A detailed examination of the limitations of this approach may be found in Ref. [8].

In the DPS contribution to the production of a W boson in association with a pair of bottom quark jets, one hard scattering produces the W via the Drell-Yan mechanism, while the other hard scattering produces a $b\bar{b}$ pair. The charged lepton from the W decay (along with the

bottom quarks in the final state) provides a relatively clean signal to tag on. Our purpose is to establish whether double parton scattering can be observed as a discernible physics process in $Wb\bar{b}$ production at LHC energies. In the rest of the paper, we outline our simulation of the DPS and SPS contributions to $Wb\bar{b}$, discuss backgrounds for the same final state, and present details of our analysis. We study various single variable and two-dimensional kinematic distributions to bring out the DPS contribution more cleanly, showing that variables designed to exploit the nature of the 2 parton to 2 parton subprocesses can be used to differentiate DPS from SPS with excellent signal over background significance, $S/\sqrt{B} \sim 10$ to 15.

2 Calculation of $Wb\bar{b}$ production

We perform all calculations at center-of-mass energy $\sqrt{s} = 7$ TeV. Event rates are quoted for 10 fb^{-1} of integrated luminosity. For the DPS case, $Wb\bar{b}$ production is computed using Eq. (2) where it is assumed that one hard scattering produces the W boson via $q\bar{q} \to W^{\pm}X$, while the other scattering produces the $b\bar{b}$ system. The individual SPS processes which make up the DPS process are generated using the POWHEG BOX event generator [9, 10, 11] which includes next-to-leading order (NLO) QCD corrections for both, plus shower emission. In the SPS production of $Wb\bar{b}$, one hard scattering produces the complete final state. The events from this process are also generated using the POWHEG BOX [12] which implements the NLO calculation of Ref. [13].

Extracting evidence for DPS $Wb\bar{b}$ production is complicated by the fact that many standard model processes imitate the $Wb\bar{b} \to b\bar{b}\ell\nu$ final state. In particular, we consider contributions from (a) top quark pair production $t\bar{t}$; (b) single top quark production ($t\bar{b}$, $\bar{t}b$, tj and $\bar{t}j$ modes); (c) Wjj, where both light jets are mistagged as b jets; and (d) Wbj where the light jet is mistagged as a b jet. We also consider the following processes, which have a negligible contribution after cuts: (a) $b\bar{b}j$ where one b quark gives an isolated lepton and the light jet is tagged as a b jet; (b) $Zb\bar{b}$ where one lepton from the Z decay is missed; and (c) $b\bar{b}b\bar{b}$ ($b\bar{b}c\bar{c}$) production where at least one heavy quark gives an isolated lepton and the other does not pass the threshold cuts. The Wjj background (where both jets fake bottom quark jets) can be produced in both SPS and DPS processes.

2.1 Simulation

We concentrate on the final state in which there are two b jets, a hard lepton, and missing transverse energy $\not{E}_T$. We consider only leptonic decays of the W boson ($W \to \ell\nu$). We focus on the case $\ell = \mu$, since electrons with low transverse momentum can be easily faked by light jets. We limit the hadronic activity in our events to include exactly two hard jets, both of which must be identified as bottom quark jets. Finally, all events (DPS and SPS $Wb\bar{b}$ as well as backgrounds) are required to pass the following acceptance cuts:

$$p_{T,b} \geq 20\,\text{GeV}\,,\ |\eta_b| \leq 2.5\,, \tag{4}$$

$$20\,\text{GeV} \leq p_{T,\mu} \leq 50\,\text{GeV}\,,\ |\eta_\mu| < 2.1\,, \tag{5}$$

$$\not{E}_T \geq 20\,\text{GeV}\,, \tag{6}$$

$$\Delta R_{b\bar{b}} \geq 0.4\,,\ \Delta R_{b\mu} \geq 0.4\,, \tag{7}$$

Process	Acceptance cuts	$\not\!\!E_T \leq 45$ GeV	$S'_{p_T} \leq 0.2$
$W^{\pm}b\bar{b}$ (DPS)	247	231	173
$W^{\pm}b\bar{b}$ (SPS)	1142	569	114
$t\bar{t}$	1428	290	13
$W^{\pm}jj$ (DPS)	43.5	37.7	27.3
$W^{\pm}jj$ (SPS)	101	55.7	19.6
Single top	492	168	15
$W^{\pm}bj$	152	53.1	8.2

Table 1: Numbers of events before and after the various cuts are applied for 10 fb^{-1} of data. After acceptance cuts, SPS $Wb\bar{b}$ production and $t\bar{t}$ production dominate the event rate. A maximum $\not\!\!E_T$ cut reduces the background from $t\bar{t}$ significantly.

where η is the pseudorapidity and ΔR_{lk} is the separation in the azimuthal-pseudorapidity plane between the two objects l and k:

$$\Delta R_{lk} = \sqrt{(\eta_l - \eta_k)^2 + (\phi_l - \phi_k)^2}\,. \tag{8}$$

The cut on the missing transverse energy $\not\!\!E_T \geq 20\,\text{GeV}$ is motivated by the fact that the neutrino momentum in W decay is not observed. The 20 GeV cut on the b jets and the lepton is invoked to eliminate contributions from the underlying event. The upper lepton p_T cut is used to reject boosted W bosons, as in the case where a W boson originates from a t-quark decay, or when the W recoils against the $b\bar{b}$ pair in SPS. Our b jet tagging efficiencies, muon identification efficiencies, fake rates, and detector resolution effects are described in Ref. [6].

Table 1 shows the number of events from the $Wb\bar{b}$ final state (DPS and SPS) and the backgrounds after the acceptance cuts, detector effects, and mistagging effects are applied (column labeled "acceptance cuts"). In these results and those that follow, we sum the W^+ and W^- events. In evaluating the DPS processes, we assume a value $\sigma_{\text{eff}} \simeq 12$ mb for the effective cross section. However, we stress that the goal is to motivate an empirical determination of its value at LHC energies. The acceptance cuts are very effective against the Wjj final states, both for DPS and SPS. The results in Table 1 make it apparent that $Wb\bar{b}$ production from SPS and the top quark pair background are the most formidable obstacles in extracting a DPS signal. We address $t\bar{t}$ background rejection in the next section.

2.2 $t\bar{t}$ background rejection

We examine three possibilities to reduce the $t\bar{t}$ background: a cut to restrict $\not\!\!E_T$ from above, rejection of events in which a top quark mass can be reconstructed, and a cut to restrict the transverse momentum of the leading jet. In the end, an upper cut on $\not\!\!E_T$ in the event appears to offer the best advantage. Indeed, one would expect that $\not\!\!E_T$ in $Wb\bar{b}$ events would be smaller than $\not\!\!E_T$ in $t\bar{t}$ events. Top quark decays give rise to boosted $W^{\pm}$'s which, after decay, should result in larger values of missing E_T compared to the $Wb\bar{b}$ process. The DPS signal is produced in the region of relatively small $\not\!\!E_T$ and the $t\bar{t}$ background has a harder spectrum in $\not\!\!E_T$. One way to suppress the $t\bar{t}$ background while leaving the DPS signal unaffected is to impose a maximum $\not\!\!E_T$ cut in the 40-60 GeV range. In the analysis that follows, we include a

maximum $\not{E}_T$ cut of 45 GeV in addition to the acceptance cuts outlined above. The effects of the maximum $\not{E}_T$ cut are shown in the third column of Table 1. This cut eliminates about 80% of the $t\bar{t}$ background that remains after the initial acceptance cuts. The cut is also effective at reducing the single top quark and Wbj backgrounds, eliminating about 67% in both cases. On the other hand, 93% of the DPS $Wb\bar{b}$ events and 50% of the SPS $Wb\bar{b}$ events are retained. Of the three possibilities we consider to reduce the $t\bar{t}$ background, a cut to restrict $\not{E}_T$ from above appears to offer the best advantage, and it is the only cut we impose in addition to the acceptance cuts specified above.

3 Separation of the DPS and SPS contributions

To separate the DPS contribution from the SPS and background contributions, it is valuable to use kinematic variables that take advantage of the 2 parton to 2 parton nature of the underlying DPS subprocesses. The observable S'_{p_T} exploits the transverse momentum balance of 2 to 2 scattering. It is defined as [4]:

$$S'_{p_T} = \frac{1}{\sqrt{2}} \sqrt{\left(\frac{|p_T(b_1, b_2)|}{|p_T(b_1)| + |p_T(b_2)|} \right)^2 + \left(\frac{|p_T(\ell, \not{E}_T)|}{|p_T(\ell)| + |\not{E}_T|} \right)^2} \,. \tag{9}$$

Here, $p_T(b_1, b_2)$ is the vector sum of the transverse momenta of the two b jets, and $p_T(\ell, \not{E}_T)$ is the vector sum of $\not{E}_T$ and the transverse momentum of the charged lepton in the final state. In DPS production, the bottom quarks are produced roughly back-to-back such that the vector sum of their transverse momenta tends to vanish. Likewise, the vector sum of the lepton and neutrino momenta tends to be small (with corrections from the boosted $W^{\pm}$). Thus, the S'_{p_T} distribution for the DPS process exhibits an enhancement at low S'_{p_T}, as shown on the left side of Fig. 2. The peak does not occur at exactly $S'_{p_T} = 0$ owing to NLO real radiation that alters the back-to-back nature of the $b\bar{b}$ and $\ell\nu$ systems. On the other hand, SPS production of $Wb\bar{b}$ does not favor back-to-back configurations; it exhibits a peak near $S'_{p_T} = 1$, a feature linked to the fact that many $b\bar{b}$ pairs are produced from gluon splitting [5].

The clean separation in S'_{p_T} between the DPS and SPS $Wb\bar{b}$ processes is obscured by the $t\bar{t}$ background, but this background can be mitigated by a maximum $\not{E}_T$ cut, as shown on the right side Fig. 2. The last column of Table 1 shows that a cut $S'_{p_T} < 0.2$ reduces the SPS $Wb\bar{b}$ rate while leaving the DPS signal relatively unaffected. In the end, the major background arises from DPS Wjj, as is expected since this process inhabits the same kinematic regions as the DPS $Wb\bar{b}$ signal. Despite this background, we find a statistical significance for the presence of DPS $Wb\bar{b}$ of $S/\sqrt{B} = 173/\sqrt{197} = 12.3$.

Azimuthal angle balance is a second notable feature of 2 parton to 2 parton scattering. Observables which take into account the angular distribution of events are also useful in the search for DPS. Figure 3 depicts two such observables. In the left plot, we show the event rates for DPS $Wb\bar{b}$ and the backgrounds (SPS $Wb\bar{b}$ included) as a function of the angle between the normals to the two planes defined by the $b\bar{b}$ and $\ell\nu$ systems. These planes are defined in the partonic center-of-mass frame and are specified by the three-momenta of the outgoing jets or leptons. The angle between the two planes is:

$$\cos \Delta\Theta_{b\bar{b},\ell\nu} = \hat{n}_3(b_1, b_2) \cdot \hat{n}_3(\ell, \nu) \tag{10}$$

where $\hat{n}_3(i, j)$ is the unit three-vector normal to the plane defined by the $i - j$ system and $b_1(b_2)$ is the leading (next-to-leading) b jet. In order to construct the normals $\hat{n}_3(b_1, b_2)$ and $\hat{n}_3(\ell, \nu)$,

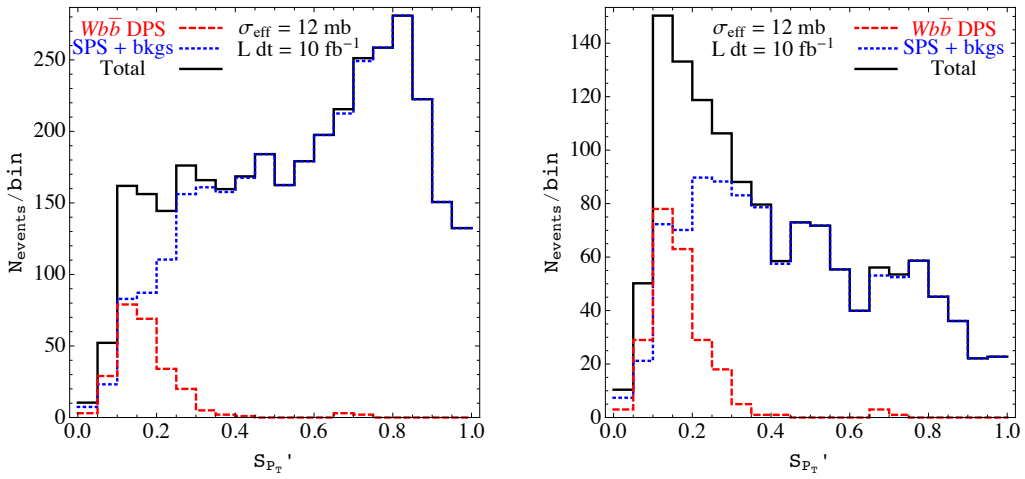

Figure 2: The S'_{p_T} distribution for DPS and SPS production of $Wb\bar{b}$ including all relevant backgrounds. On the left, only the minimal acceptance cuts are imposed, while, on the right, an additional maximum $\not{E}_T$ cut is imposed ($\not{E}_T < 45$ GeV). A maximum $\not{E}_T$ cut greatly reduces the background and produces a sharp peak in the region of small S'_{p_T} where DPS is expected to dominate.

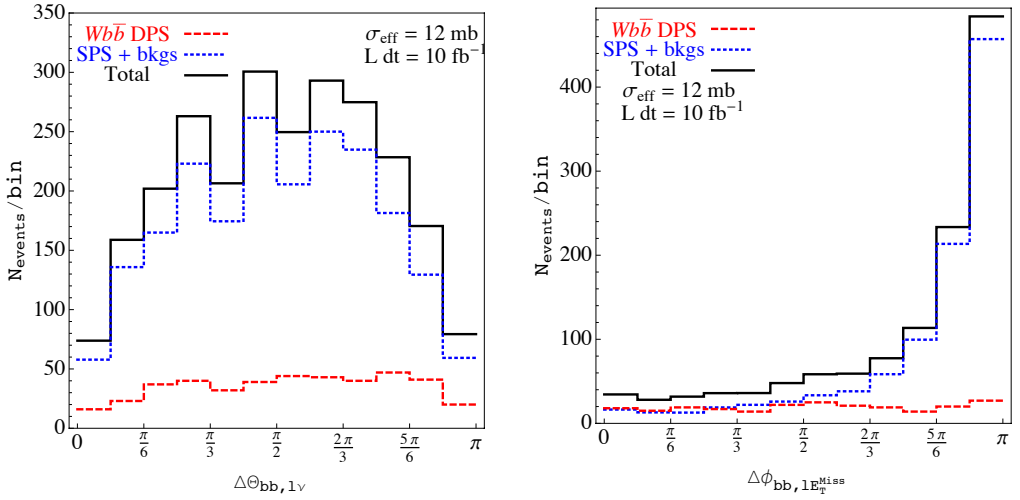

Figure 3: The event rate as a function of the angle between the normals of the two planes defined by the $b\bar{b}$ and $\ell\nu$ systems (left), and the azimuthal angle between the transverse momentum vectors of the $b\bar{b}$ and $\ell\not{E}_T$ systems (right). In SPS events, it is apparent that there is a strong correlation in the angles.

we require full event reconstruction using the on-shell W-boson mass relations. We see that the distribution of the DPS events is rather flat, aside from the cut-induced suppressions at

$\Theta_{b\bar{b},\ell\nu} \sim 0$ and $\sim \pi$, whereas the SPS events show a strong correlation, with a distribution that peaks near $\Delta\Theta_{b\bar{b},\ell\nu} \sim \frac{\pi}{2}$.

In the right plot of Fig. 3, we show the event rates as a function of the azimuthal angle between the transverse momentum vectors of the $b\bar{b}$ and $\ell \not{E}_T$ systems. Since this azimuthal angle is defined in the transverse plane, it requires only $\not{E}_T$. Full event reconstruction to determine the neutrino momentum is not needed. The DPS distribution is flat while the SPS distribution shows a strong correlation, with a preference for values toward π.

The DPS and SPS samples exhibit different behavior as a function of angular observables. However, the dominance of SPS $Wb\bar{b}$ and backgrounds over DPS $Wb\bar{b}$ for the full range of these observables makes it impossible to extract a DPS signal from these distributions by themselves. Having found interesting features in the transverse momentum variable S'_{p_T} and in the angular distributions, we now put this information together in a two-dimensional distribution.

4 Two-dimensional distributions

.

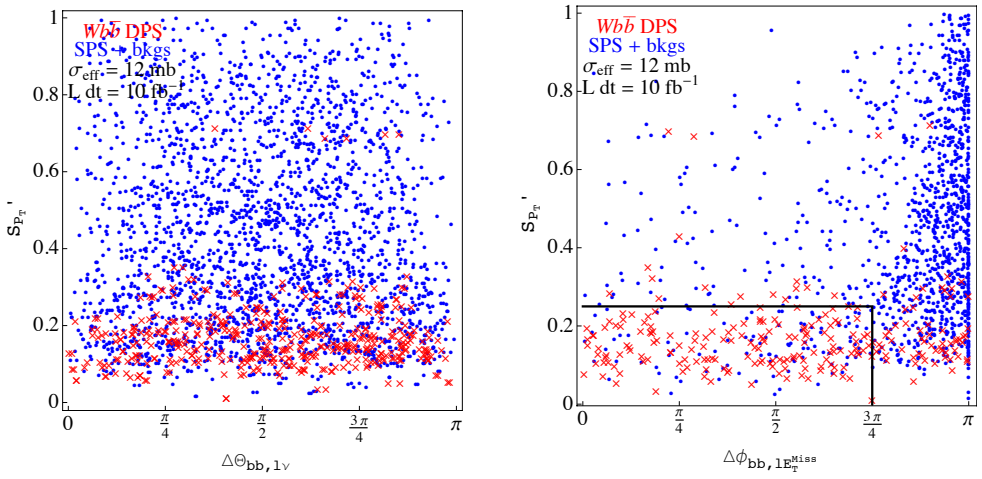

Figure 4: Two-dimensional distributions of events in the variables (left) S'_{p_T} and $\Delta\Theta_{b\bar{b},\ell\nu}$, and (right) S'_{p_T} and $\Delta\phi_{bb,\ell\not{E}_T}$. In both cases, the $Wb\bar{b}$ DPS events (denoted by red **x**) lie in the lower half of the plane, while the $Wb\bar{b}$ SPS and background events (denoted by blue **dots**) occupy the upper half. The plot on the right appears to achieve a cleaner separation.

Two-dimensional distributions of one variable against another show distinct regions of DPS dominance (or SPS and background dominance). In Fig. 4, we construct two such scatter plots. On the left, we show S'_{p_T} versus the angle between the normals of the two planes defined by the $b\bar{b}$ and $\ell\nu$ systems ($\Delta\Theta_{b\bar{b},\ell\nu}$). The DPS events reside predominantly in the lower half of the plane (small S'_{p_T}) and are distributed evenly in the angular variable. The separation between DPS $Wb\bar{b}$ and the SPS component is not as pronounced in the $S'_{p_T} - \Delta\Theta_{b\bar{b},\ell\nu}$ plane as we saw in our earlier study of $b\bar{b}jj$ [5]. In the $Wb\bar{b}$ case, the background events are more evenly distributed over the full plane, to some extent resulting from inclusion of both solutions for

the neutrino's longitudinal momentum in the $W^{\pm}$ decay. (The greater density of points in the left plot of Fig. 4 relative to the right plot is explained by the fact that both solutions for the neutrino momentum are included in the left plot).

On the right of Fig. 4, we show the two-dimensional distribution of S'_{p_T} and $\Delta\phi_{bb,\ell\ \not{E}_T}$. This distribution shows a high degree of separation between the DPS $Wb\bar{b}$ and the SPS plus background samples. To quantify the degree of separation, we define a region in this plane that gives the highest statistical significance. Restricting $S'_{p_T} < 0.25$ and $\Delta\phi_{bb,\ell\ \not{E}_T} < 3\pi/4$, we find a a sample of 154 signal and 103 background events, corresponding to a statistical significance of $S/\sqrt{B} = 15.2$. Employing the scatter plot in S'_{p_T} and $\Delta\phi_{bb,\ell\ \not{E}_T}$, we achieve a better significance than from S'_{p_T} alone. As long as the maximum value of $\Delta\phi_{bb,\ell\ \not{E}_T}$ is in the $\pi/2$-$3\pi/4$ range, a statistically significant extraction of DPS $Wb\bar{b}$ from the other events can be obtained, given our assumed effective cross section $\sigma_{\rm eff} = 12$ mb and luminosity.

In this study of $Wb\bar{b}$, as in our earlier study of $b\bar{b}jj$, we find that DPS can be important relative to SPS in specific parts of phase space. We suggest experimental analyses of $Wb\bar{b}$ at the LHC in terms of the two-dimensional distributions presented in this section, with the goal to establish whether a discernible DPS signal is found. Assuming success, the p_T dependence of the leading object and other properties of these DPS events can be examined to establish whether the expected properties of DPS are seen. The enriched DPS event sample can be used for a direct measurement of the effective cross section $\sigma_{\rm eff}$. Data are needed.

Acknowledgments. The work reported here was done in collaboration with Chris Jackson, Seth Quackenbush, and Gabe Shaughnessy. It was supported financially by the U. S. Department of Energy under Contract No. DE-AC02-06CH11357.

References

[1] Axial Field Spectrometer Collaboration, Z. Phys. C **34** (1987) 163.

[2] UA2 Collaboration, Phys. Lett. B **268** (1991) 145-154.

[3] CDF Collaboration, Phys. Rev. D **56** (1997) 3811-3832.

[4] D0 Collaboration, Phys. Rev. D **81** (2010) 052012 [arXiv:0912.5104 [hep-ex]].

[5] E. L. Berger, C. B. Jackson and G. Shaughnessy, Phys. Rev. D **81** (2010) 014014 [arXiv:0911.5348 [hep-ph]].

[6] E. L. Berger, C. B. Jackson, S. Quackenbush and G. Shaughnessy, Phys. Rev. D **84** (2011) 074021 [arXiv:1107.3150 [hep-ph]].

[7] P. Bartalini, E. L. Berger, B. Blok, G. Calucci, R. Corke, M. Diehl, Y. L. Dokshitzer, L. Fano *et al.*, arXiv:1111.0469 [hep-ph].

[8] M. Diehl, D. Ostermeier and A. Schafer, JHEP **1203** (2012) 089 arXiv:1111.0910 [hep-ph].

[9] P. Nason, JHEP **0411** (2004) 040 [arXiv:hep-ph/0409146].
S. Frixione, P. Nason and C. Oleari, JHEP **0711** (2007) 070 [arXiv:0709.2092 [hep-ph]].
S. Alioli, P. Nason, C. Oleari and E. Re, JHEP **1006** (2010) 043 [arXiv:1002.2581 [hep-ph]].

[10] S. Alioli, P. Nason, C. Oleari and E. Re, JHEP **0807** (2008) 060 [arXiv:0805.4802 [hep-ph]].

[11] S. Frixione, P. Nason and G. Ridolfi, JHEP **0709** (2007) 126 [arXiv:0707.3088 [hep-ph]].

[12] C. Oleari and L. Reina, JHEP **1108** (2011) 061, [Erratum-ibid. **1111**, 040 (2011)] [arXiv:1105.4488 [hep-ph]].

[13] F. Febres Cordero, L. Reina and D. Wackeroth, Phys. Rev. D **74** (2006) 034007 [hep-ph/0606102].